DEUTSCHES ELEKTRONEN-SYNCHROTRON

DESY

DESY 64/8
Mai 1964
Experimente

PION PRODUCTION WITHOUT ANNIHILATION IN ANTIPROTON PROTON INTERACTIONS AT 3.6 GeV/c

by

H.C. Dehne, E. Lohrmann, E. Raubold, P. Söding,
M.W. Teucher, and G. Wolf
Physikalisches Staatsinstitut, II. Institut für
Experimentalphysik, Hamburg
and
Deutsches Elektronen-Synchrotron DESY, Hamburg

2 HAMBURG-GR. FLOTTBEK 1, NOTKESTIEG 1

PION PRODUCTION WITHOUT ANNIHILATION IN ANTIPROTON PROTON INTERACTIONS AT 3.6 GeV/c

by

H.C. Dehne, E. Lohrmann, E. Raubold, P. Söding,
M.W. Teucher, and G. Wolf
Physikalisches Staatsinstitut, II. Institut für
Experimentalphysik, Hamburg
and
Deutsches Elektronen-Synchrotron DESY, Hamburg

Abstract:

Interactions of antiprotons were studied at a momentum of 3.6 GeV/c in a hydrogen bubble chamber. Particular attention was paid to single and multiple pion production without annihilation. Cross sections for the various pion production channels are given. The total cross section for pion production without annihilation and not including strange particle production is $18.6 \,^{+\,2.4}_{-\,3.3}$ mb. Single pion production is found to agree with the predictions of the one pion exchange model for small values of the four-momentum transfer. Double pion production in the reaction $\bar{p}p \to p\bar{p}\pi^+\pi^-$ agrees with the one pion exchange model for all values of the four-momentum transfer, if all possible diagrams are taken into account. The main contribution comes from events, where a 3/2 3/2 pion nucleon isobar antiisobar pair is produced. For these events the Treiman Yang angular distribution and the decay angular distributions of the isobars are also in agreement with the one pion exchange model.

I. INTRODUCTION

Many details of the antiproton-proton interaction have been established at incident energies >1 GeV mainly by bubble chamber studies, but also by other techniques [1-13]. Whereas at low energies the annihilation channel dominates the character of the interaction, the importance of the non-annihilation channels increases with increasing energy. Pion production in $\bar{p}p$ interactions without annihilation has been studied at 1.6 GeV/c [1,14] and between 3 and 4 GeV/c [8,9,10,15,16]. We present here a fairly systematic investigation of these processes at 3.6 GeV/c. The measurements can be compared with measurements of pion production by proton collisions which have been carried out at about the same energy [17,18].

Among the attempts to gain a certain theoretical understanding of the experimental results for pp and $\bar{p}p$ collisions in the GeV region the one pion exchange model (OPEM) has been very popular [19,20,21]. In contrast to many other applications of OPEM, the pp and $\bar{p}p$ interaction offers a fairly straightforward experimental check, since all coupling constants and cross sections which enter in the calculations are known. Strictly speaking, this is true only in the pole approximation, which neglects off-shell effects. As is well known, this approximation gives rather bad agreement with experiment in many cases, even for small values of the square of the four-momentum transfer Δ^2. Of the attempts to improve the situation, we shall follow here Ferrari and Selleri. They modified the pole approximation by introducing multiplicative correction functions for the pion propagator and the vertex functions. These correction functions depend essentially only on Δ^2 and have a much weaker dependance on Δ^2 than the pion propagator. Once they have been found by comparison with measurements at a specific energy, they can be used to predict the results of experiments at other energies and involving different reactions. The theory contains then no adjustable parameters and gives for example absolute values of cross sections.

Ferrari and Selleri [22] had remarkable success in fitting pion production in pp interactions between 1.6 GeV/c and 3.7 GeV/c with a unique choice of these correction functions. The same functions should be valid for $\bar{p}p$ interactions, leading to a definite prediction for the measurements.

$\bar{p}p$ and pp pion production processes are different in three important respects:

(1) Final state interactions are different (annihilation),

(2) The reactions have a different symmetry character (Pauli principle for the protons),

(3) In the two reactions different isospin states are involved.

If in spite of these differences the OPEM would give a good description of the $\bar{p}p$ interaction this would be a strong argument for a dominant contribution of one pion exchange both for pp and $\bar{p}p$ interactions. Experimental studies of this problem were carried out by several authors. The CERN group, studying single pion production in $\bar{p}p$ interactions at 3 and 4 BeV found that the OPEM gives too large a value for the total single pion production cross section by roughly a factor of 2 [8,10]. A similar result was reached by Baltay et al.[9] at 3.25 GeV/c. For double pion production, Baltay et al. found good agreement with the OPEM for events with small momentum transfer and for the total cross section. In a previous communication [23] we found good agreement for single and double pion production at 3.6 GeV/c, provided one restricts oneself to small values of the four-momentum transfer. In this paper we shall present a more detailed and more general comparison.

II. EXPERIMENTAL PROCEDURE

The measurements were made on a sample of 14400 photographs from the Saclay 81 cm hydrogen bubble chamber exposed to an electrostatically separated beam [24] of antiprotons from the CERN proton synchrotron. The beam momentum was 3.6 GeV/c.

The contamination of the beam was determined from the photographs by looking for high energy knock-on electrons produced by beam tracks [25]. In this experiment it gave the ratio (pions + muons)/(all beam particles) = 0.149 $\pm$ 0.010. The fraction of pions was determined by looking for interacting beam particles with a knock-on electron with momentum $>$ 16 MeV/c. This gave a ratio (pions/all beams tracks) = 0.015 $\pm$ 0.015.

The total cross section was determined from the number of events and beam tracks inside a certain fiducial volume. Most of the film was scanned 3 independent times. A hydrogen density of 0.0602 gcm^{-3} was used. A detailed account of all corrections made has been published previously [26].

The total number of two- and four prong events measured in this experiment was 2216. The measurements were carried out in all three views, using digitized projectors. A maximum detectable momentum of $>$ 250 GeV/c was determined from measurements on beam tracks in photographs without magnetic field. For the spacial reconstruction of the tracks the geometry program WELAGA written by G. Wolf and H. Schneider was used. The kinematic fitting was done by GRIND [27]. We tried to identify all tracks with momenta $<$ 1.8 GeV/c by their ionisation, either visually or by measurement of the mean gap length [28, 29]. This information prooved to be very valuable for deciding on the correct hypothesis for an event.

The identification was done in the following way. An interpretation of a particular event was considered established if it fulfilled all of the following three conditions:

(1) It must be consistent with the ionization.
(2) χ^2 from the kinematic fitting by GRIND must be smaller than a certain limit. This limit was $\chi 2 < 14$ for elastic events, $\chi 2 < 30$ for 4-prong events without neutral particles, and $\chi 2 < 6$ for events with one neutral particle. For events with more than one neutral particle, the missing mass had to have a consistent value.

(3) All other possible interpretations must be ruled out.
An interpretation was considered ruled out, if it fulfilled one or more of the following criteria:

(1) It was inconsistent with ionization by > 2.5 standard deviations,
(2) For an interpretation with no or one neutral particle, there was no corresponding fit in GRIND.
(3) If the interpretation involved more than one neutral particle, it was inconsistent with the missing 4-momentum.

Fig. 1 shows the $\chi 2$ distribution for elastic and inelastic 2-prong events, fig. 2 for 4-prong events.

There were of course events, for which no single unambiguous interpretation was obtained. They were treated in the following way: For 2-prong events, it was checked if the momentum and lab angle of the positively charged particle satisfied the relation expected for elastic scattering. A certain fraction of these could be unambiguously identified as elastic in this way. For the remaining (2- and 4-prong) events the true interpretation was considered unknown, and the limits of error for the partial cross sections include the uncertainty of the interpretation in these cases.

In particular, the following numbers are upper limits on the possible contamination of the most interesting reactions by other channels:

(1) $\bar{p}p \longrightarrow \bar{p}\,p\,\pi^{o}$: contamination < 15 %, mainly by $\bar{p}p \longrightarrow \pi^{+}\pi^{-}\pi^{o}\pi^{o}\ldots$

(2) $\bar{p}p \longrightarrow \bar{n}\,p\,\pi^{-}$: contamination < 2o %, mainly by $\bar{p}p \longrightarrow \pi^{+}\pi^{-}\pi^{o}\pi^{o}\ldots$

(3) $\bar{p}p \longrightarrow \bar{p}\,n\,\pi^{+}$: contamination not known, therefore not used for differential cross sections

(4) $\bar{p}p \longrightarrow \bar{p}\,p\,\pi^{+}\pi^{-}$: contamination < 5 %.

III. CROSS SECTIONS

A summary of the cross sections obtained is given in table I.

A principal difficulty in obtaining the cross section for multiple pion production without annihilation is caused by the presence of the channel $\bar{p}p \longrightarrow \bar{n}n$ + pions, which cannot be distinguished from annihilation, if no additional information (e.g. secondary interactions) is known.

In the case of the 2 prong reaction $\bar{p}p \longrightarrow \bar{n}n\pi^{+}\pi^{-}$ ($\pi^{o}\ldots$), an upper limit of 4.5 mb was obtained from the observed number of events involving π^{+} and π^{-} and having a missing mass larger than 2 nucleon masses. The contribution of the annihilation reaction $\bar{p}p \longrightarrow \pi^{+}\pi^{-}\pi^{o}\pi^{o}$ ($\pi^{o}\ldots$) to this sample of events was estimated with the help ofastatistical model from the observed number of reactions $\bar{p}p \longrightarrow \pi^{+}\pi^{-}\pi^{o}\pi^{o}$ ($\pi^{o}\ldots$) in which the missing mass was smaller than 2 nucleon masses and which thus could be uniquely identified as annihilations. This led to a cross section of 2.5 mb for the non-annihilation channel $\bar{p}p \longrightarrow \bar{n}n\pi^{+}\pi^{-}$ ($\pi^{o}\ldots$). This value was however only used to get a most probable value of the inelastic cross section. The errors given for this cross section include the uncertainty coming from the contamination from the annihilation channel.

For the reaction $\bar{p}p \longrightarrow \bar{n}n\pi^+\pi^-\pi^+\pi^-$ (π^0...), an upper limit to the cross section of 0.6 mb was obtained by using the information contained in the missing mass.

The cross section for non-annihilation reactions with ≥ 6 charged outgoing particles was estimated from the ionization of the outgoing tracks, and by comparison with the statistical model and with pp interactions at 3.67 GeV/c [18], to be < 0.15 mb.

In order to get the total non-annihilating pion production cross section, one also has to estimate the contribution to the cross section coming from 0-prong events (i.e., events with only neutral outgoing particles). This estimate was made using the number of antineutron interactions, electron-positron pairs and neutral strange particle decays related to 0-prong events. The detection efficiency for antineutrons was 1.5 %. We assumed that all 5 or 7 prong events were due to $\bar{n}p$ annihilation and that the $\bar{n}p$ and $\bar{p}p$ cross sections for annihilation were equal [30] at the energies considered. Various sources of background were checked and found to be negligible. From the antineutron stars, we obtained for the sum of the cross sections ($\bar{p}p \longrightarrow \bar{n}n, \bar{n}n\pi^0$ (π^0...)) the value $(3.9 \pm {}^{0.3}_{1.4})$ mb.

From the electron-positron-pairs assoziated with 0-prong events the average number of π^0 mesons emitted from these interactions was found to be 0.55 ± 0.15. This suggests a large relative contribution of elastic charge exchange $\bar{p}p \longrightarrow \bar{n}n$ to the 0-prong events [31]. If one estimates the average number of neutral pions produced in an annihilation $\bar{p}p \longrightarrow \pi^0\pi^0$ (π^0...), from the statistical model, and the π^0 multiplicity in the reaction $\bar{p}p \longrightarrow \bar{n}n\pi^0$ (π^0...) from camparison with the charged mode $\bar{p}p \longrightarrow \bar{p}p\pi^0$ (π^0...), one gets as upper limits 0.8 mb for 0-prong annihilation and 3.0 mb for inelastic charge exchange. In addition one may also estimate the absolute number of π^0's produced in the 0-prong annihilations using the statistical model.

The remaining number of neutral pions would then correspond to a cross section of 2.1 mb for the inelastic charge exchange reaction.

IV. SINGLE PION PRODUCTION

The total cross sections are given in table 1, the branching ratio is

$$\frac{2\sigma(\bar{p}p\pi^0)}{\sigma(\bar{n}p\pi^-)+\sigma(\bar{p}n\pi^+)} = 0.78 \pm 0.17$$

The statistical model gives 0.80, the pure $I = \frac{3}{2}$ isobar model 2 and the one pion exchange model (see sec. VI) 0.85 for this ratio. In the region of incident antiproton momenta of 1.6 GeV/c to 4 GeV/c, this branching ratio is found to decrease from 1.69 to 0.76 [1,10].

Only the two channels

$$\bar{p}\,p \longrightarrow \bar{p}\,p\,\pi^0$$
$$\longrightarrow \bar{n}\,p\,\pi^-$$

were studied in more detail. The differential cross section $d\sigma / d\Delta^2$ is shown in fig. 3, Δ^2 being the square of the four-momentum transfer between the initial and final nucleon. Comparison with the phase space shows a strong predominance of small Δ^2. The region of small Δ^2 is separately exhibited in fig. 3 where one sees that $d\sigma / d\Delta^2$ rises from 0 to a maximum value which is reached at about $\Delta^2 \simeq 2\mu^2$, μ is the mass of the pion. In fig. 4, $d\sigma / dM^*$ is given as a function of M^*, the mass of the pion-antinucleon system, with the additional restriction to events with small $\Delta^2 < 7\mu^2$, for which an unambiguous discrimination against annihilation was possible. Comparison with phase space shows the influence of the $I=J=\frac{3}{2}$ pion antinucleon resonance.

V. MULTIPLE PION PRODUCTION

The following final states are possible for non-annihilation processes leading to 4 charged outgoing particles:

$$\bar{p}\,p \longrightarrow \begin{array}{l} \bar{p}p\,\pi^+\pi^- \\ \bar{p}p\,\pi^+\pi^-\pi^0\ (\pi^0\ldots) \\ \bar{n}p\,\pi^-\pi^+\pi^-\ (\pi^0\ldots) \\ \bar{p}n\,\pi^+\pi^-\pi^+\ (\pi^0\ldots) \\ \bar{n}n\,\pi^+\pi^-\pi^+\pi^-\ (\pi^0\ldots) \end{array}$$

We concentrated on the first of these reactions, which has by far the largest cross section. 455 events corresponding to this reaction were found.

The mass distributions of the combinations $p\pi^+$, $\bar{p}\pi^-$, $p\pi^- + \bar{p}\pi^+$ for the reaction $\bar{p}\,p \longrightarrow \bar{p}\,p\,\pi^+\pi^-$ are schown in fig.5 a, b,c. The importance of the formation of the $I=J=\frac{3}{2}$ pion nucleon isobar and anti-isobar is clearly seen. The peak value is at 1.220 GeV, the full width at half maximum is 12o MeV. This is in good agreement with observations made at 3.25 GeV/c [15].

The distribution of the $\pi^+\pi^-$ mass is also shown in fig. 5d. There is no evidence for the production of the ρ meson. The mass distribution of the combination $p\pi^+\pi^-$ and $\bar{p}\,\pi^-\,\pi^+$ is given in fig. 5e. Since for the small values of Δ^2 the double isobar production predominates, the distribution is given separately for events with $\Delta^2 > 0.3$ GeV^2. This eliminates 65% of the double isobar production. Δ^2 is the square of the 4-momentum transfer between initial nucleon and final $p\pi^+$ system. For the further discussion, we denote the masses of the $p\,\pi^+$ and $\bar{p}\,\pi^-$ systems by M_1^* and M_2^* respectively, and define the $I=J=\frac{3}{2}$ isobar region by $1.13\ \text{GeV} \leq M_1^* \leq 1.33$ GeV.

Evidence for simultaneous isobar - antiisobar production can be obtained from a scatter plot M_1^* versus M_2^*.

The cross section for double isobar formation was obtained by subtracting in the scatter plot the phase space contribution of four uncorrelated particles. The phase space was normalized in the region outside the $I=J=\frac{3}{2}$ resonance, i.e. 1.48 GeV $\leq (M^*_1, M^*_2) \leq$ 1.88 GeV. We find $\sigma(\bar{p}p \longrightarrow \bar{N}^* N^*) = 2.13 \pm 0.13$ mb. This is 56% of the total cross section for the reaction $\bar{p}p \longrightarrow \bar{p}p\pi^+\pi^-$. (In the more extended isobar region 1.12 GeV $\leq (M^*_1, M^*_2) \leq$ 1.38 GeV used by Ferbel et al. [15], we get a cross section of 2.45 ± 0.15 mb in agreement with their value of 2.6 ± 0.3 mb at 3.25 GeV/c.)

Fig. 6 shows the distribution of Δ^2, which is strong evidence for the peripheral nature of the reaction. The distribution of the transverse momentum p_T and of the longitudinal momentum p_L of the $\bar{p}\,\pi^-$ system in the overall center-of-mass system is given in fig. 7. We find a mean value $\langle p_T \rangle = 0.339$ GeV/c. In about 3% of the events the $\bar{p}\,\pi^-$ system goes backwards in the CMS.

The following tests [32] for charge conjugation (C) and for CP invariance were made: CMS angular distribution of π^+ vs. π^- and of p vs. $\bar{p}$, mass distribution of the $p\pi^+$ system vs. $\bar{p}\,\pi^-$, and azimuthal angle $\phi_{p\pi^+}$ vs. $\phi_{\bar{p}\pi^-}$, fig. 8. For all distributions tested, the agreement with C and CP invariance is above the 5% confidence level.

Fig. 9 shows the distribution of the angle between the two normals of the decay planes for the isobar and the antiisobar, evaluated in the overall CMS. The distribution is shown for several upper limits of Δ^2. All the distributions are consistent with isotropy.

Of the reactions with 3 pions in the final state, the channel $\bar{p}p \longrightarrow \bar{p}p\pi^+\pi^-\pi^0$ is the easiest one to identify and was therefore the only one studied in detail. There were 59 events of this type.

From the mass distribution for different particle combinations, the following conclusions can be drawn:

(a) In contrast to the strong occurrence of the $I=J=\frac{3}{2}$ isobar in double pion production, no (anti)isobar formation was found.

(b) The $\pi^+\pi^-$ mass distribution follows phase space.

(c) The $\pi^+\pi^-\pi^0$ mass distribution shows the production of the ω meson. We estimate the cross section for $\bar{p}p \longrightarrow \bar{p}p\omega$ to be $(60 \pm 20)\,\mu b$. This agrees with the cross section found for $pp \longrightarrow pp\omega$ at about the same energy [33]. No clear evidence of η production was found.

VI. DISCUSSION IN TERMS OF THE ONE PION EXCHANGE MODEL

The dominance of small 4-momentum transfers in single and double pion production suggests an interpretation in terms of peripheral processes. Therefore the OPEM contribution to these processes were calculated and are here compared with the experimental results.

The contributing one pion exchange graphs shown in fig. 1o can be calculated in a straightforward way in terms of the pion-nucleon coupling constant and pion nucleon cross sections. It is well known, however, that the experiments do not agree well with this pion pole contribution, but that allowance must be made for the fact that one is observing these processes for values of the invariant four-momentum transfer Δ^2 which are a considerable distance away from the one pion pole at $\Delta^2 = -\mu^2$. In their work on one pion exchange in nucleon - nucleon interactions, Ferrari and Selleri [34] argued that the pole term should be modified by a multiplicative form factor which may involve corrections to the proper pion-nucleon vertex ($F(\Delta^2)$), corrections to the pion propagator ($F'(\Delta^2)$) and finally corrections to the pion-nucleon scattering vertices taking into account the off-the-mass-shell charakter of the exchanged pion. They have shown that

in the region of the $I=J=\frac{3}{2}$ resonance the off-shell pion nucleon scattering amplitude is equal to the on-shell (physical) amplitude times a certain function $F(\Delta^2)\cdot\psi(M^*,\Delta^2)$. Here M^* is the pion - nucleon mass, $F(\Delta^2)$ the vertex correction factor, and $\psi(M^*,\Delta^2)$ a function which they have explicitely calculated (see (22), equ. 4.1 thru 4.4). Contrary to $\psi(M^*,\Delta^2)$, the functions $F(\Delta^2)$ and $F'(\Delta^2)$ can at present only be determined by comparison with experiment.

Thus there are apart from the pole expressions the following overall multiplicative form factors in the amplitudes:

for diagramms (a), (b) (fig.10): $F^2(\Delta^2).F'(\Delta^2)\cdot\psi(M^*,\Delta^2)$ (1)

for diagramms (c), (d) : $F^2(\Delta^2).F'(\Delta^2).\psi(M_1^*,\Delta^2)\cdot\psi(M_2^*,\Delta^2)$ (2)

where Δ^2 is the square of the four-momentum of the exchanged pion. For diagramms (e) and (f) there is no corresponding theoretical argument. The unknown function $F^2(\Delta^2).F'(\Delta^2)$ of Δ^2 has been determined by Ferrari and Selleri by a comparison of the OPEM prediction for the processes $pp \longrightarrow pn\pi^+$, $pp \longrightarrow pp\pi^0$ with the experimental results between 1.6 and 3.7 GeV/c [17,35,36]. Remarkable agreement was found at all energies with the unique choice:

$$F^2(\Delta^2)\cdot F'(\Delta^2) = 0.72\left[1+\frac{\Delta^2+\mu^2}{4.73\mu^2}\right]^{-1} + 0.28 \quad (3)$$

For pion - nucleon mass values M^* outside the region of the first resonance, the above arguments for off-shell pion nucleon scattering are not valid. There are, however, arguments [22] that the ratio of the on-shell to the off-shell pion nucleon elastic amplitude depends mainly on Δ^2 and only weakly on M^*, so that a reasonable approximation should be to replace $\psi(M^*,\Delta^2)$ by an unknown function of Δ^2 only. Accordingly, with an approximation of the form

$$F^2(\Delta^2).F'(\Delta^2).\psi(M^*,\Delta^2) \simeq \left[1+\frac{\Delta^2+\mu^2}{\gamma}\right]^{-1} \quad (4)$$

for the overall form factor for single pion production, Ferrari

and Selleri [22,37] tried to fit the above mentioned pp reactions for all M^* and got good agreement in the whole energy region, choosing $\gamma \approx 90\mu^2$. This one-pole approximation for the form factor shows that the form factor constitutes only a small correction to the pion pole contribution, since it corresponds to a pole at a distance $\approx 90\mu^2$.

In the present work we used function (2), inserting (3) for $F^2(\Delta^2)\, F'(\Delta^2)$ in the calculation of the amplitude of diagram (c) (fig.10), because there the main contribution comes from pion nucleon masses inside the first resonance. For $\bar{p}p \longrightarrow \bar{p}p\pi^+\pi^-$, one must consider both diagrams (c) and (d). In the "double isobar region" for diagram (c) however, (d) contributes only 1.0% and therefore in an earlier paper [23] only the dominant graph (c) was considered. In this paper we have also included the contribution of diagram (d).

For the calculation of (a) and (b), we took the form factor (4) trying different values of the cut-off parameter γ. This was done because even if one restricts oneself to, say, small four-momentum transfers to the proton, i.e. small Δ^2 for diagram (a), then still (b) contributes significantly according to the calculations and for (b) also large values of Δ^2 occur in the integration.

Finally, for diagrams (e) and (f) (fig. 10) we took (4) as form-factor [38] with $\gamma = 90\mu^2$.

A further approximation made in the calculations was to neglect the interference between different partial waves in the virtual pion nucleon scattering. The unmeasurable cross section for $\pi^0 p \longrightarrow p\pi^+\pi^-$ needed for the evaluation of diagrams (e) and (f) was taken from the discussion in reference (38). For the momentum and angular distribution of the secondary π^-, needed to get the $\bar{p}$, $(\bar{p}\pi^-)$ momentum transfer, plausible assumptions were made guided by experiments of Kirz [39] and

Newcombe [40]. Possible interference terms between (c), (d), (e) and (f) were neglected.

The comparison with the experimental results for single pion production is given in figs. 3 and 4. One gets good agreement for $d\sigma/d\Delta^2$ and $d\sigma/d M^*$, if the cutoff γ introduced by the form factor is at $90\mu^2 \leq \gamma \leq 120\mu^2$ and if the square of the four-momentum transfer Δ^2 to the proton is small. The branching ratio $\sigma(\bar{p}p\pi^0)/\sigma(\bar{n}p\pi^-) = 1.12 \pm 0.23$ for $\Delta^2 < 7\mu^2$ is also in agreement with the prediction 1.15 of the OPEM.

While there is good agreement for small four-momentum transfers, the OPEM cross section is too large for $\Delta^2 \gtrsim 25\mu^2$, as is shown in fig. 3. It is not possible to force agreement by choosing a smaller cutoff parameter in our case. This is because even for small four-momentum transfers to the nucleon, i.e. small values for the square of the four-momentum Δ^2 of the exchanged pion in diagram (a), the contributions from diagram (b) where the virtual pion may have a relatively large Δ^2 are not negligible. Therefore, if one tries to get agreement also for large Δ^2 by adjusting γ, one gets disagreement for small Δ^2. The total cross sections given by the OPEM ($\gamma = 90\Delta^2$) are 3.23 mb for $\bar{p}p \longrightarrow \bar{p}p\pi^0$ and 3.80 mb for $\bar{p}p \rightarrow \bar{n}p\pi^-$ differing roughly by a factor of 1.6 from the measured values.

For double pion production in the reaction $\bar{p}p \longrightarrow \bar{p}p\pi^+\pi^-$ the comparision with the OPEM is made in fig. 6 which shows the distribution $d\sigma/d\Delta^2$. Here Δ^2 is the square of the four-momentum transfer between the initial proton and the final $p\pi^+$ system. It should be noted that the Δ^2 distribution shown is not the square of the four-momentum of the exchanged pion in the case of the "Drell graphs" (e) (f). This representation was chosen in order to be able to present all data in one figure.

There is quantitative agreement for all values of Δ^2 between the experimental data and the sum of all contributions from graphs (c), (d), (e) and (f). No parameter has been adjusted. Table 2 gives more detailed information for the Δ^2 dependance of the

various cross sections. As is seen, the "double isobar diagram" (c) predominates for small Δ^2. This has been pointed out in an earlier paper [23] and by Baltay et al. [9].

Fig. 11 shows the combined $p\pi^+$ and $\bar{p}\pi^-$ mass distributions. The Drell graphs (e) and (f) contribute 23 % in the isobar region, and only 8 % in the double isobar region, but contribute practically all of the cross section for $p\pi^+$ or $\bar{p}\pi^-$ masses > 1.4 GeV. If one limits oneself to events with $\Delta^2 < 0.3$ GeV^2, the mass distribution is completely described by the double isobar graph (see remark above.)

The predominance of double isobar production provides a further check for the OPEM, if one considers the decay angular distribution of the isobars in their CMS. In case of real pion nucleon scattering in the $I=J=\frac{3}{2}$ state, one expects a distribution of the form $1 + 3\cos^2\theta$ for the angle θ between the incoming and outgoing (anti) proton in the (anti) isobar CMS. If the observed angular distribution is averaged out over the resonance region, one gets instead a distribution of the approximate form $1+2.5\cos^2\theta$ due to interference with small $J=\frac{1}{2}$ contributions.

We combined the experimental angular distribution for the $p\pi^+$ and $\bar{p}\pi^-$ systems in the double isobar region (1.13 GeV $\leq (M_1^*, M_2^*) \leq 1.33$ GeV), with restriction to various upper limits in Δ^2. The distributions were fitted with a polynomial of the form $1 + B\cos\theta + C\cos^2\theta$. Fig. 12 and table 3 show the results. The forward-backward ratio, shown also in table 3, is consistent with the value 1. The distribution obtained with the restriction $\Delta^2 \leq 0.15$ GeV^2 is in agreement with the expected distribution $1 + 2.5\cos^2\theta$ with a χ^2 - probability of 30%.

A further test for pion exchange is provided by the distribution of the Treiman-Yang angle [41]. In the region of Δ^2 and M^*, where the double isobar graph is expected to dominate, this angle is defined as the angle between $(p_{out} \times \pi^+)$ and $(\bar{p}_{in} \times (\bar{p}_{out}+\pi-))$ in the laboratory system. Another independent Treiman-Yang angle

may be defined in the $\bar{p}$ rest system in an analogous way. The distributions were plotted with the restriction of the $p\pi^+$ and $\bar{p}\pi^-$ systems to be in the isobar region, and $\Delta^2 \leq 0.3$ GeV^2. The distributions were consistent with isotropy with a χ^2 probability of 60%.

It has recently been suggested that all simple single particle exchange models should be corrected for absorptive processes [42]. In principle a correction of this kind should undoubtedly be made, however, the numerical estimate of such effects given in [42] leads to very substantial changes in the predictions of such models. In particular, one could expect quite different corrections for pp and $\bar{p}p$ interactions, since the absorptive behaviour is different. If this would be so, the agreement of all our distributions with the OPEM, and in particular the agreement with predictions based on the pp reactions [17, 18, 35, 36] would probably have to be ascribed to a chande coincidence.

VII. CONCLUSIONS

From the present study of pion production without annihilation in $\bar{p}p$ interactions at 3.6 GeV/c, we may draw the following conclusions:

(1) The total inelastic (non-annihilation) cross section not including (anti) hyperon production is $18.6 \pm {}^{2.4}_{3.3}$ mb. This is smaller than the inelastic cross section found for pp interactions [17,18] at about the same energy (26.5 mb). It may be compared with the result of Baltay et al.[9] for $\bar{p}p$ interactions at 3.25 GeV/c (14.0mb) and of Lynch et al.[1] and Hinrichs et al.[30] at 1.61 GeV/c (5.1 mb)

(2) The most prominent pion production channel is $\bar{p}p \rightarrow \bar{p}p\pi^+\pi^-$, which is strongly favoured by the formation of two $I=J=\frac{3}{2}$ pion (anti)nucleon resonant states. This reaction was first observed by Ferbel et al. [15]. 56% of the

events of this channel proceed via "double isobar formation".

(3) No indication of production of ϱ or η mesons was found.

The cross section for $\bar{p}p \longrightarrow \bar{p}p\omega$ is 0.06 ± 0.02 mb and agrees with the cross section for $pp \longrightarrow pp\omega$ at about the same energy [33].

(4) An application of the OPEM with Ferrari - Selleri form factors to single pion production leads to agreement with experiment within statistics, if the square of the four - momentum transfer Δ^2 to the nucleon is restricted to $\Delta^2 < 7\,\mu^2$. With this restriction, we find agreement with the absolute (not normalized) distribution $d\sigma/d\Delta^2$. Also the distribution of the antinucleon pion effective mass is consistent with the OPEM. For larger values of Δ^2, the experimental cross sections are smaller than those from the OPEM. This agrees with similar observations of Lynch et al. [1] at 1.61 GeV/c. Accordingly, the total single pion production cross section is smaller than predicted by the OPEM by a factor of the order of 2. The same result has also been obtained by the CERN group [8, 10] at 3.0 GeV/c and 4.0 GeV/c and by Baltay et al. [9] at 3.25 GeV/c.

(5) Double pion production in the reaction $\bar{p}p \longrightarrow \bar{p}p\,\pi^+\pi^-$ agrees perfectly with the OPEM for all values of the four - momentum transfer, if all possible one pion exchange graphs are taken into account. In particular, this holds for $d\sigma/d\Delta^2$, for the distribution of the (anti)nucleon pion effective mass, for the Treiman-Yang angular distribution and for the decay angular distribution of the pion nucleon isobar. The main contribution is given by the "double isobar diagram" (fig.1o c). Similar conclusions were reached by Baltay et al. [9] at 3.25 GeV/c. The total cross section found is 3.80 ± 0.22 mb, the OPEM predicts 3.55 mb.

Acknowledgements

We are very grateful to the CERN proton synchrotron and track chamber groups and to the Saclay bubble chamber groups for the photographs, and to Drs. E. Ferrari, Y. Goldschmidt-Clermont, D.R.O. Morrison, and J. Sandweiss for valuable discussions and comments. The great help of many people of our laboratory, especially of E. Burkhard, D. Cords, G. Knies, P. Schilling and D. Wandschneider is also gratefully acknowledged. We thank the Institut für Plasmaphysik in München-Garching, the Deutsches Rechenzentrum in Darmstadt, and the Rechenzentrum at DESY for allowing us to use their IBM computers. This work was supported by the Bundesministerium für wissenschaftliche Forschung.

References:

1. The most complete study has been made by the ALVAREZ group at 1,61 GeV/c. For a list of references to this work, see for instance, G.R. Lynch, R.E. Foulks, G.R. Kalbfleisch, S. Limentani, J.B. Shafer, M.L. Stevenson and N.H.Xuong, Phys.Rev. 131, 1276 (1963)

2. R. Armenteros, C. A. Coombes, B. Cork, G.R. Lamberton and C.A. Wenzel, Phys. Rev. 119, 2o68 (1960)

3. G. von Dardel, D.H. Frisch, R. Mermod, R.H.Milburn, P.A. Piroué, M. Vivargant, G. Weber and K. Winter, Phys.Rev. Lett. 5, 333 (1960)

4. S.J. Lindenbaum, W.A. Love, J.A. Niederer, S. Ozaki, J.J. Russel and L.C.L. Yuan, Phys. Rev. Lett. 7, 185 (1961)

5. K.J. Foley, S.J. Lindenbaum, W.A. Love, S. Ozaki, J.J.Russel, L.C.L. Yuan, Phys. Rev. Lett. 11, 503 (1963)

6. U. Amaldi jr., T. Fazzini, G. Fidecaro, C. Ghesquière, M. Legros and H. Steiner, Nuovo Cim. to be published.

7. T. Ferbel, J. Sandweiss, H.D. Taft, M.Gailloud, T.W.Morris, R.M. Lea, T.E. Kalogeropoulos, Proceedings of the International Conference on High Energy Physics at CERN. 1962, p.76

8. Y. Goldschmidt-Clermont, M. Guinea, T. Hofmokl, R.Lewish, D.R.O. Morrison, M. Schneeberger and S. Unamuno, Proceedings of the International Conference on High Energy Physics at CERN, 1962, p.84

9. C. Baltay, T. Ferbel, J. Sandweiss, H.D.Taft, B.B.Culwick, W.B. Fowler, M. Gailloud, J.K. Kopp, H.I.Louttit, T.W.Morris, J.R. Sanford, R.P. Shutt, D.L. Stonehill, R. Stump,A.M. Thorndike, M.S. Webster, W.J. Willis, A.H. Bachmann,P.Baumel, R.M. Lea, Proceeding of the Stanford Nucleon Structure Meeting, June 1963

10. O. Czyzewski. B. Escoubès, Y. Goldschmidt-Clermont, M. Guinea-Moorhead, T. Hofmokl, R. Lewisch, D.R.O. Morrison, M. Schneeberger and S. Unamuno, Proceedings of the Siena Conference on Elementary Particles, 1963

11. C. Baltay, J. Sandweiss, H.D. Taft, B.B. Culwick, W.B. Fowler, J.K. Kopp, R.I. Louttit, J.R.Sanford, R.P. Shutt, D.L. Stonehill, A.M. Thorndike and M.S. Webster, Proceedings of the International Conference on high Energy Physics at CERN, 1962, p.233
Phys. Rev. Lett. 11, 32 (1963)
Phys. Rev. Lett. 11, 346 (1963)

12. R. Armenteros, E. Fett, B. French, L. Montanet, V. Nikitin, S. Szeptycka, Ch. Peyrou, R. Böck, A. Shapira, J. Badier, L. Blaskovicz, B. Equier, B. Gregory. F. Muller, S.J. Goldsack, D.H. Miller, C.C. Butler, B. Tallini, J. Kinson, L. Riddiford, A. Levegue, J. Meyer, A. Verglas, S. Zylberach, Proceedings of the International Conference on High Energy Physics at CERN, 1962, p.236

13. B. Musgrave, G. Petmezas, L. Riddiford, R. Böck, E. Fett, B.R. French, J.B. Kinson, Ch. Peyrou, M. Szeptycka, J.Badier, M. Bazin, L. Blaskovic, B. Egner, J. Huc. S.R. Borenstein, S.J. Goldsack, D.H. Miller, J. Meyer, D. Revel, B. Tallini and S. Zylberach, Nuovo Cimento to be published.

14. G.R. Lynch, Reviews of Mod. Phys. 33, 395 (1961)

15. T. Ferbel, J. Sandweiss, H.D. Taft, M. Gailloud, T.E. Kalogeropoulos, T.W. Morris and R.M. Lea, Phys. Rev. Lett. 9, 351 (1962) T. Ferbel, thesis 1963

16. H.C. Dehne, E. Lohrmann, E. Raubold, P. Söding, M.W.Teucher and G. Wolf, Proceedings of the Siena Conf. on Elementary Particles, 1963

17. - G.A. Smith, H. Courant, E.C. Fowler, H. Kraybill, J. Sandweiss and H. Taft, Phys. Rev. 123, 2160 (1961)

18. - E.L. Hart, R.I. Louttit, D. Luers, T.W. Morris, W.J.Willis and S.S. Yamamoto, Phys. Rev. 126, 747 (1962)

19. - G.F. Chew and F.E. Low, Phys. Rev. 113, 1640 (1959)

20. - F. Salzmann and G. Salzmann, Phys. Rev. 125, 1703 (1962)

21. - E. Ferrari and F. Selleri, Suppl. Nuovo Cim.24, 453 (1962)

22. - E. Ferrari and F. Selleri, Nuovo Cim. 27, 1450 (1963)

23. - H.C. Dehne, E. Raubold, P. Söding, M.W. Teucher, G.Wolf and E. Lohrmann, Phys. Lett. 9, 185 (1964)

24. - S. van der Meer, CERN report 60-22 (1960) CERN report 63-3 (1963)

25. - H. Djerassi, M. Lami, A. Accensi and G. Coignet, CERN/TC/ Physics/62/2, 1962 (unpublished)

26. - B. Escoubès, A. Fedrighini, Y. Goldschmidt-Clermont, M. Guinea-Moorhead, T. Hofmokl, R. Lewisch, D.R.O.Morrison, M. Schneeberger, S. de Unamono, H. C. Dehne, E. Lohrmann, E. Raubold, P. Söding. M.W. Teucher, and G. Wolf, Phys.Lett. 5, 132 (1963)

27.- R. Böck, GRIND 709, Kinematics Program Manual, unpublished

28. - N.N. Biswas, I. Derado, K. Gottstein, V.P. Kenney, D. Luers, G. Lütjens and N. Schmitz, Nuclear Instr. 20, 135 (1962)

29. - B. Sechi-Zorn and G.T. Zorn, Suppl. Nuovo Cim. 26, 197 (1963) and references given there.

30. - C.K. Hinrichs, B.J. Moyer, J.A. Poirier and P.M.O. Ogden, Phys. Rev. 127, 617 (1962)

31. - At the somewhat lower incident momentum of 3.0 GeV/c the CERN group has measured the cross section for elastic charge exchange directly with the result 2.4 ± 0.7 mb (ref. 10)

32. - A. Pais, Phys. Rev. Lett. 3, 242 (1959)

33. - E.L. Hart, R.I. Louttit and T.W. Morris, Phys. Rev. Lett. 9, 133, (1962)

34. - E. Ferrari and F. Selleri, Nuovo Cim. 21, 1028 (1961)

35. - W.J. Fickinger, E. Pickup, D.K. Robinson and E.O.Salant, Phys. Rev. 125, 2082 (1962)

36. - D.V. Bugg, A.J. Oxley, J.A. Zoll, J.G. Rushbroke, V.E. Barnes, J.B. Kinson, W.P. Dodd, G.A. Doran and L. Riddiford, Phys. Rev. 133, B 1017 (1964)

37. - E. Ferrari and F. Selleri, Phys. Rev. Lett. 7, 387 (1961)

38. - E. Ferrari, Nuovo Cim. 30, 240 (1963)

39. - J. Kirtz, thesis, UCRL 10720 (1963)

40. - P. Newcombe, thesis, UCRL 10563 (1962)

41. - S.B. Treimann and C.N. Yang, Phys. Rev.Lett. 8, 140 (1962)

42. - L. Durand, III, and Yam Tsi Chin, Phys.Rev. Lett. 12, 399 (1964)

Table I. Cross sections.

Reaction		Cross section (mb)	
$\bar{p}p \longrightarrow$	all channels	76.2 ± 1.8	
	$\bar{p}p$	20.9 ± 0.8	
	$\bar{p}p\pi^0$	1.9 ± 0.3	
	$\bar{n}p\pi^-$	2.6 ± 0.4	
	$\bar{p}n\pi^+$	2.2 ± 0.4	a)
	$\bar{p}p\pi^-\pi^+$	3.8 ± 0.2	
	$\bar{p}p\pi^+\pi^-\pi^0$	0.6 ± 0.1	
	$\bar{p}p\omega$	0.06 ± 0.02	
	$\bar{n}p\pi^+\pi^-\pi^-$	0.5 ± 0.3	
	$\bar{p}n\pi^-\pi^+\pi^+$	0.6 ± 0.3	
	single pion production, total	$8.7 \pm \begin{matrix}1.1\\2.1\end{matrix}$	
	multiple pion production, total	$9.8 \pm \begin{matrix}2.1\\2.6\end{matrix}$	
	total pion production	$18.6 \pm \begin{matrix}2.4\\3.3\end{matrix}$	

a) C invariance is used to determine this cross section.

T A B L E II.

Total cross sections for $\bar{p}p \longrightarrow \bar{p}p\pi^+\pi^-$. The values predicted by OPEM are compared with the experimental values for several upper limits in the square of the four-momentum transfer Δ^2 between initial p and final $p\pi^+$ system. (c),(d),(e),(f) denote the contributions of the different diagrams in Fig. 1o.

Δ^2/GeV^2	σ(OPEM) (mb) (c),(d)	(e),(f)	total	σ (Expt.)(mb)
≤ 0.2	1.02	0.07	1.09	1.09 ± 0.10
≤ 0.3	1.44	0.17	1.61	1.79 ± 0.13
≤ 0.5	1.75	0.43	2.18	2.38 ± 0.15
all	2.04	1.51	3.55	3.80 ± 0.22

T A B L E III.

Reaction $\bar{p}p \longrightarrow \bar{p}p\pi^+\pi^-$ coefficients of a fit $1 + B\cos\theta + C\cos^2\theta$ to the decay angular distribution of the isobar and antiisobar and the forward/backward ratio f/b of the decay(anti-) proton in the (anti-) isobar rest system for several upper limits in the square of the four-momentum transfer Δ^2 between p and $p\pi^+$ isobar.

	$\Delta^2 \leq 0.30 GeV^2$	$\Delta^2 \leq 0.20 GeV^2$	$\Delta^2 \leq 0.15\ GeV^2$
B	0.16 ± 0.12	0.21 ± 0.19	0.35 ± 0.31
C	0.89 ± 0.29	1.67 ± 0.51	2.48 ± 0.86
f/b	1.13 ± 0.11	1.09 ± 0.14	1.13 ± 0.19

FIGURE CAPTIONS

Fig. 1 χ^2-distributions for 2-prong events of type (a) $\bar{p}p \rightarrow \bar{p}p$ and (b) $\bar{p}p \longrightarrow \bar{p}p\pi^o$, $\bar{p}p \rightarrow \bar{n}p\pi^-$.

Fig. 2 χ^2-distributions for 4-prong events of type (a) $\bar{p}p \longrightarrow pp\pi^+\pi^-$ and (b) $\bar{p}p \rightarrow \bar{p}p\,\pi^+\pi^-\pi^o$.

Fig. 3 Sum of differential cross sections for $\bar{p}p \longrightarrow \bar{p}p\,\pi^o$ and $\bar{p}p \longrightarrow \bar{n}p\pi^-$ as a function of Δ^2, the square of the four-momentum transfer to the proton. Curve (α) is phase space, (β) is the OPEM prediction without a form factor ("pole approximation") (γ) OPEM using a form factor with an effective cutoff at $\gamma = 90\,\mu^2$. The region $\Delta^2 < 10\,\mu^2$ is separately exhibited. The number of events is 125. For $\bar{p}p\,\pi^o$, also the distribution of the invariant momentum transfer to the antiproton is included (assuming C invariance). For the absolute cross section every event has been counted only once.

Fig. 4 Sum of differential cross sections for $\bar{p}p \longrightarrow \bar{p}p\,\pi^o$ and $\bar{p}p \longrightarrow \bar{n}p\,\pi^-$ as a function of the mass M^* of the final antinucleon pion system with simultaneous restriction of the invariant momentum transfer $\Delta^2 < 7\,\mu^2$. (90 events). Curve (α) is phase space, (β) is the OPEM prediction without a form factor ("pole approximation"), (γ) OPEM using a form factor with an effective cutoff at $\gamma = 90\,\mu^2$.

Fig. 5 Mass spectra for $\bar{p}p \longrightarrow \bar{p}p\pi^+\pi^-$ of the combinations (a) $p\pi^+$, (b) $\bar{p}\pi^-$, (c) $p\pi^-$ and $\bar{p}\pi^+$ combined, (d) $\pi^+\pi^-$, (e) $p\pi^+\pi^-$ and $\bar{p}\pi^+\pi^-$ combined. Curves are phase space, normalized to events outside

the isobar region for (a) and (b), and to all events for (c). In (d) and (e) the phase space curve is corrected for the production of pairs of isobars at the rate observed, assuming isotropic decay of the isobars. In (e) the mass distributions for events with $\Delta^2 > 0.3$ GeV^2 is separately exhibited (dashed lines), with Δ^2 being the squared four-momentum transfer between initial p and final $p\pi^+$ system.

Fig. 6 Reaction $\bar{p}p \longrightarrow \bar{p}p\pi^+\pi^-$; distribution of the square of the four-momentum transfer Δ^2 between incident proton and final $p\pi^+$ system. Curves (α), (β) and (γ) are the OPEM-prediction (not normalized) using diagrams (c) + (d), (e) + (f) and (c) + (d) + (e) + (f) (fig.10), respectively.

Fig. 7 Distribution of the longitudinal (a) and transverse (b) momentum of the $\bar{p}\pi^-$ system in the overall CMS for $\bar{p}p \longrightarrow \bar{p}p\pi^+\pi^-$.

Fig. 8 Reaction $\bar{p}p \longrightarrow \bar{p}p\pi^+\pi^-$. Distribution of the azimuthal angle ϕ between the two particles $p\pi^+$ (a) and $\bar{p}\pi^-$(b). ϕ ($p\pi^+$) is defined as the angle in the overall CMS between the projections of the p and π^+ momenta on a plane perpendicular to the momentum of the incident $\bar{p}$, going from p to π^+ in the positive direction. CP invariance requires identity of the distributions of ϕ ($p\pi^+$) and ϕ ($\bar{p}\pi^-$), C invariance of the ϕ ($p\pi^+$) and ($2\pi - \phi$ ($\bar{p}\pi^-$)) distribution (ref. (32)).

Fig. 9 Distribution of the angle η between the normals of the decay planes of the isobar and the antiisobar in the overall CMS, for the reaction $\bar{p}p \longrightarrow \bar{p}p\pi^+\pi^-$(with restriction of the masses of $p\pi^+$ and $\bar{p}\pi^-$ to the "isobar region"). (a), (b), (c) correspond to events

having squared four-momentum transfer Δ^2 between p and $p\pi^+$ smaller than 0.30, 0.20 and 0.15 GeV^2, re - spectively.

Fig. 10 One pion exchange diagrams taken into account in the calculations.

Fig. 11 Reaction $\bar{p}p \longrightarrow \bar{p}p\pi^+\pi^-$. Distributions of the mass M^* for the $p\pi^+$ and $\bar{p}\pi^-$ systems $d\sigma/dM^* = 1/2 \cdot (d\sigma/dM^*_1 + d\sigma/dM^*_2)$. Curves ($\alpha$), ($\beta$) and ($\gamma$) are the OPEM results due to graphs (c) + (d), (e) + (f) and (c)+(d)+(e)+(f) (Fig.10), respectively.

Fig. 12 Reaction $\bar{p}p \longrightarrow \bar{p}p\pi^+\pi^-$. Distribution of the angle between the momenta of the incident and the final proton in the rest system of the final $p\pi^+$ system, combined with the corresponding angular distribution of the $\bar{p}\pi^-$ system. The masses of both the $p\pi^+$ and the $\bar{p}\pi^-$ systems are simultaneously restricted to the 3/2-3/2 isobar region (1.13 GeV $\leq M^* \leq$ 1.33 GeV). Different upper limits of the square of four-momentum transfer Δ^2 between initial p and final $p\pi^+$ system are employed as indicated.

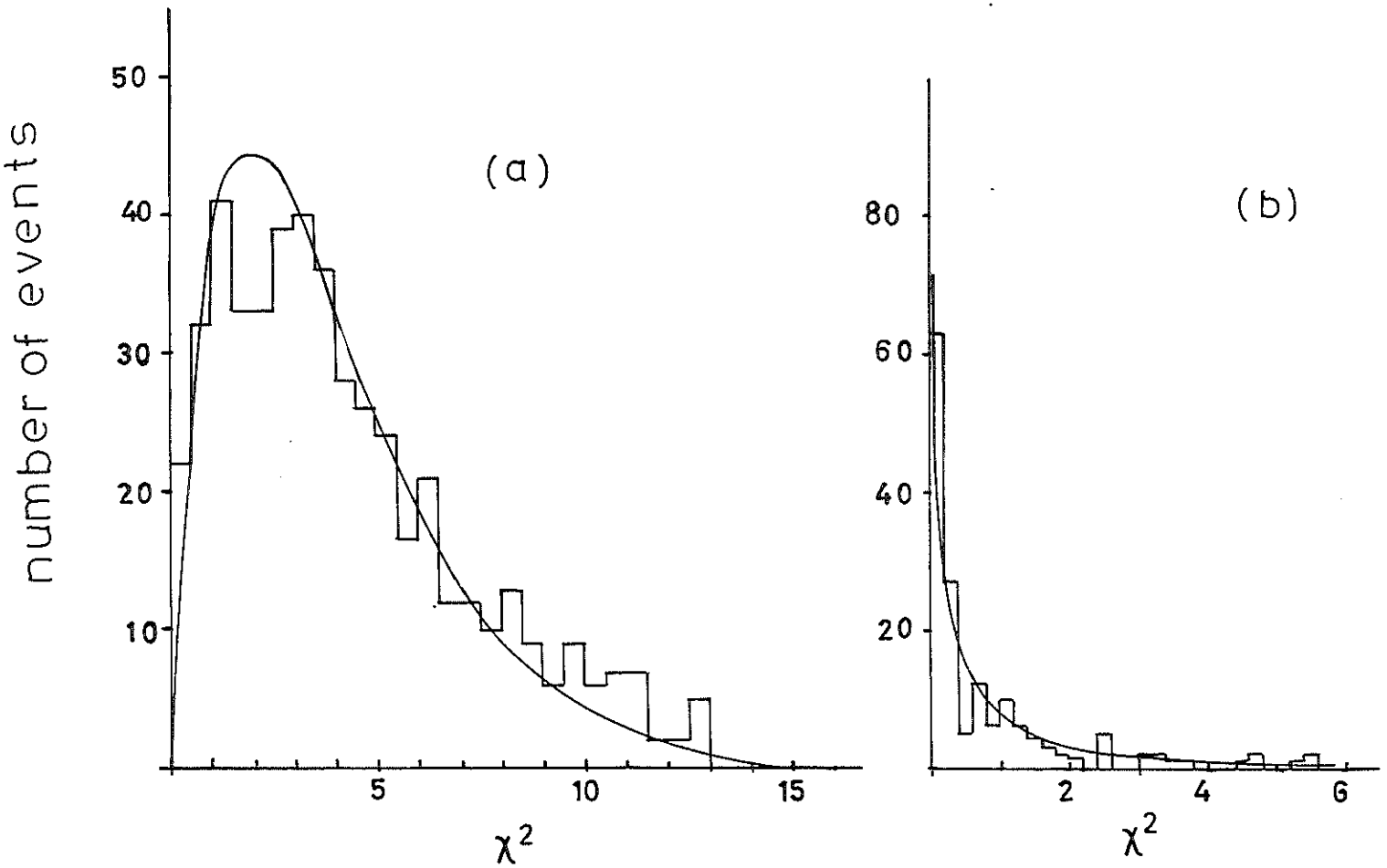
number of events
50
40
30
20
10
(a)
5
10
15
χ^2
80
60
40
20
(b)
2
4
6
χ^2

Fig. 1

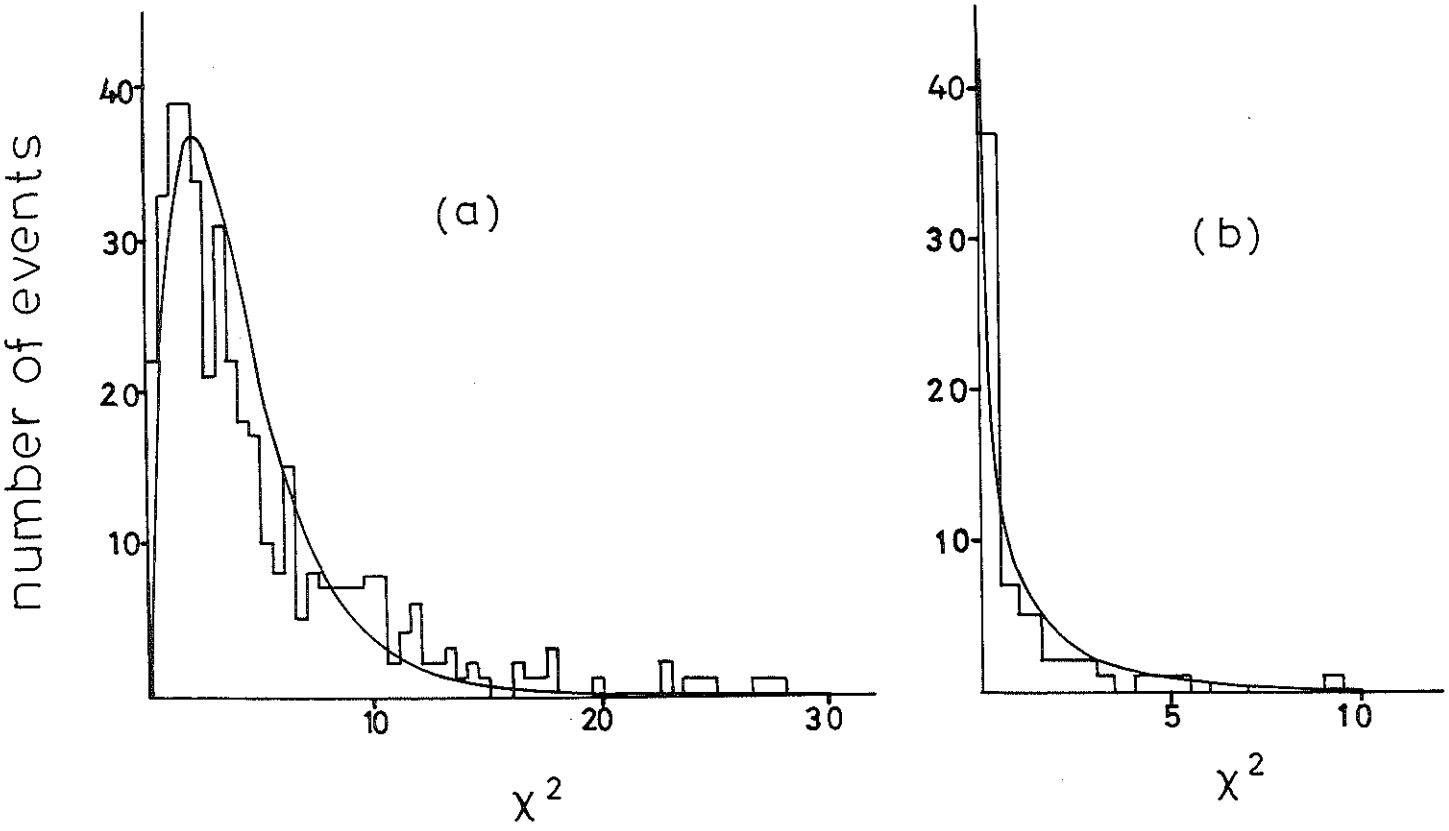

Fig 2

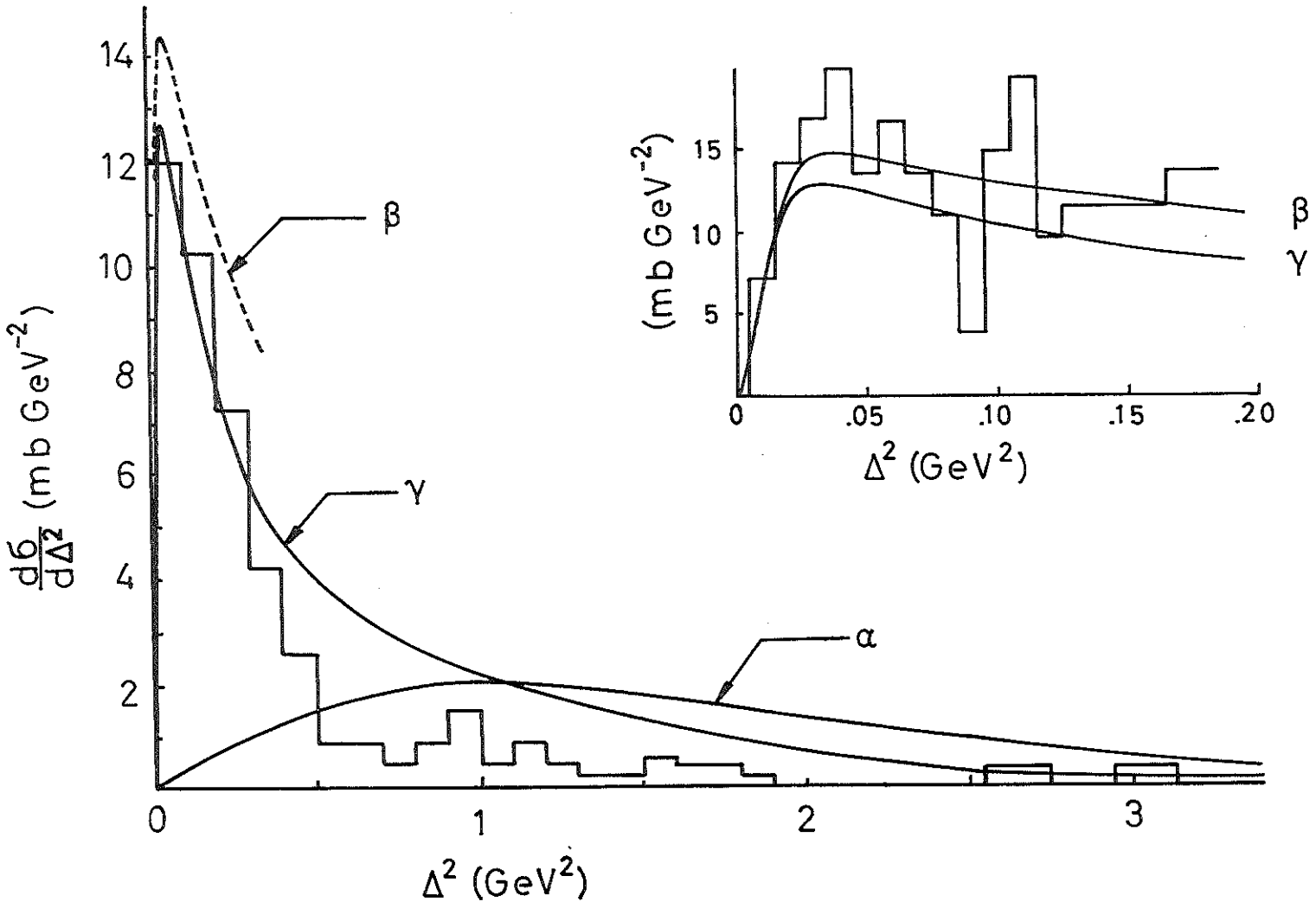
14
12
10
8
6
4
2
0
1
2
3
$\frac{d\sigma}{d\Delta^2}$ (mb GeV^{-2})
Δ^2 (GeV^2)
β
γ
α
15
10
5
(mb GeV^{-2})
0
.05
.10
.15
.20
Δ^2 (GeV^2)
β
γ

Fig 3

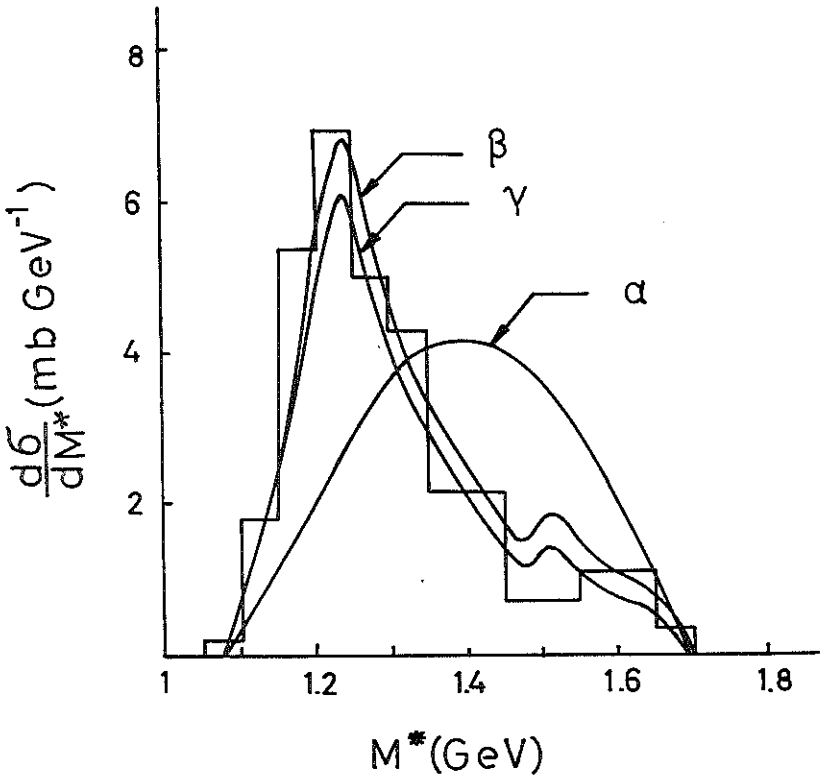

Fig 4

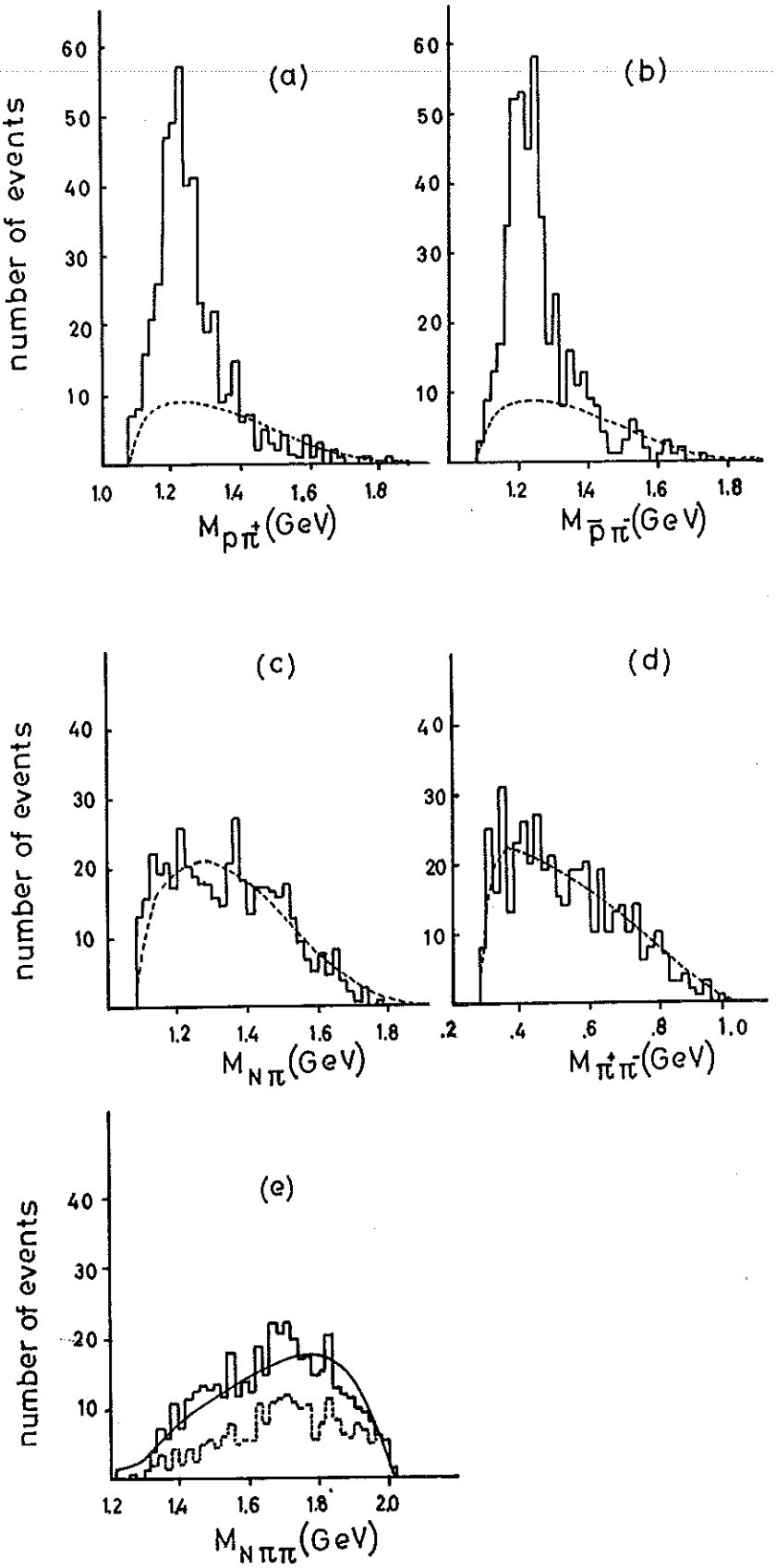
(a)
(b)
(c)
(d)
(e)
number of events
$M_{p\pi^+}$(GeV)
$M_{\bar{p}\pi^-}$(GeV)
$M_{N\pi}$(GeV)
$M_{\pi^+\pi^-}$(GeV)
$M_{N\pi\pi}$(GeV)

Fig. 5

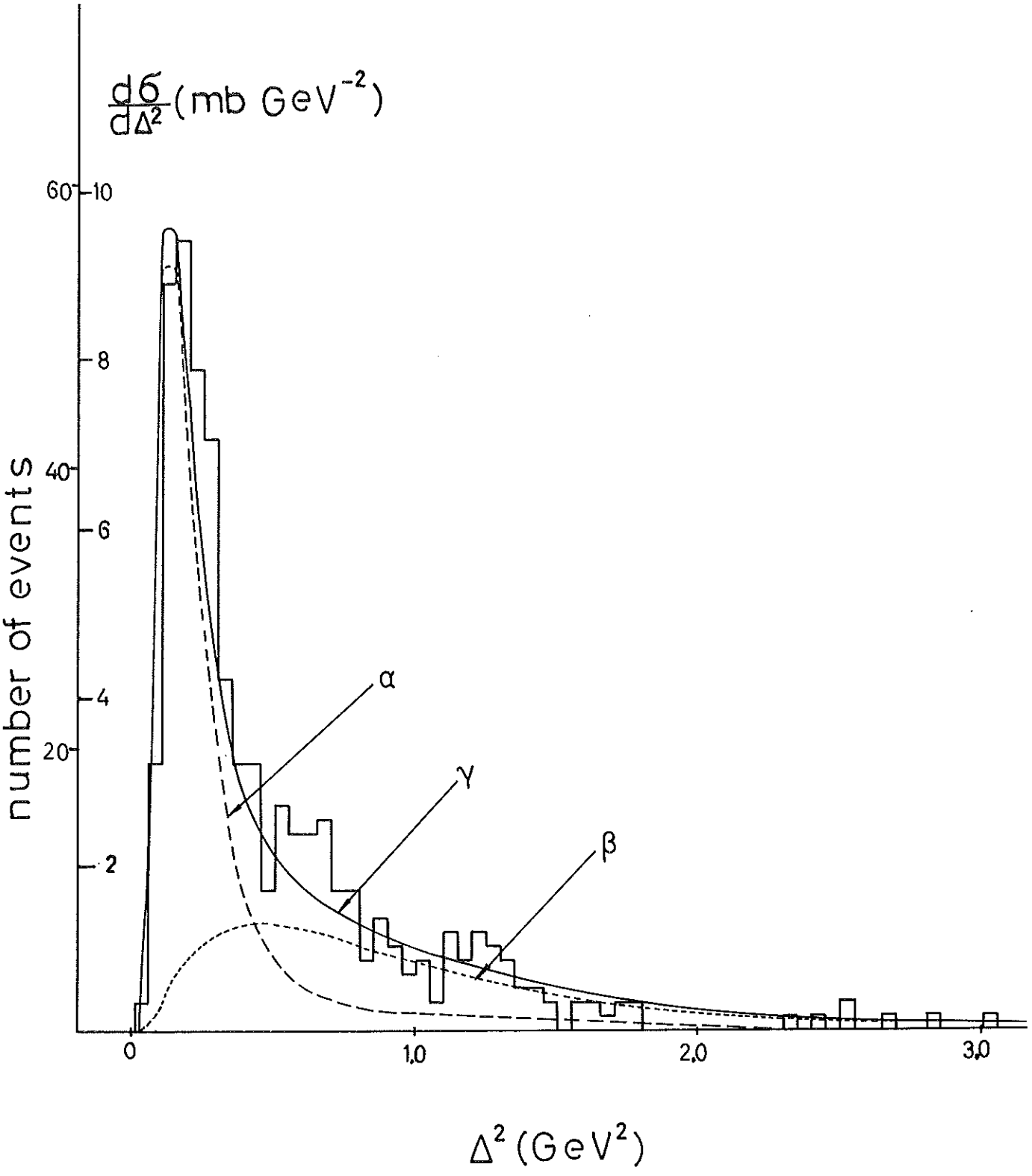
$\frac{d\sigma}{d\Delta^2}$ (mb GeV^{-2})
number of events
60
40
20
10
8
6
4
2
0
1,0
2,0
3,0
α
γ
β
Δ^2 (GeV^2)

Fig. 6

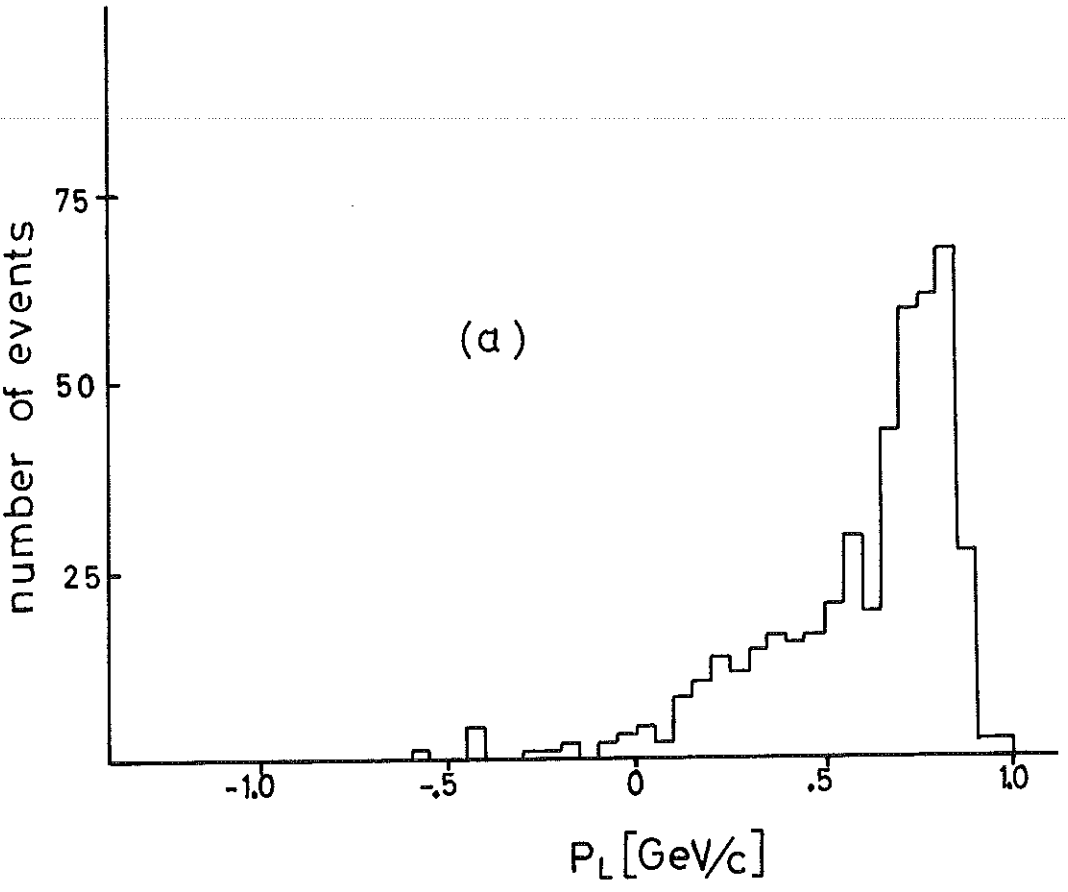
(a)
number of events
75
50
25
-1.0
-.5
0
.5
1.0
P_L [GeV/c]

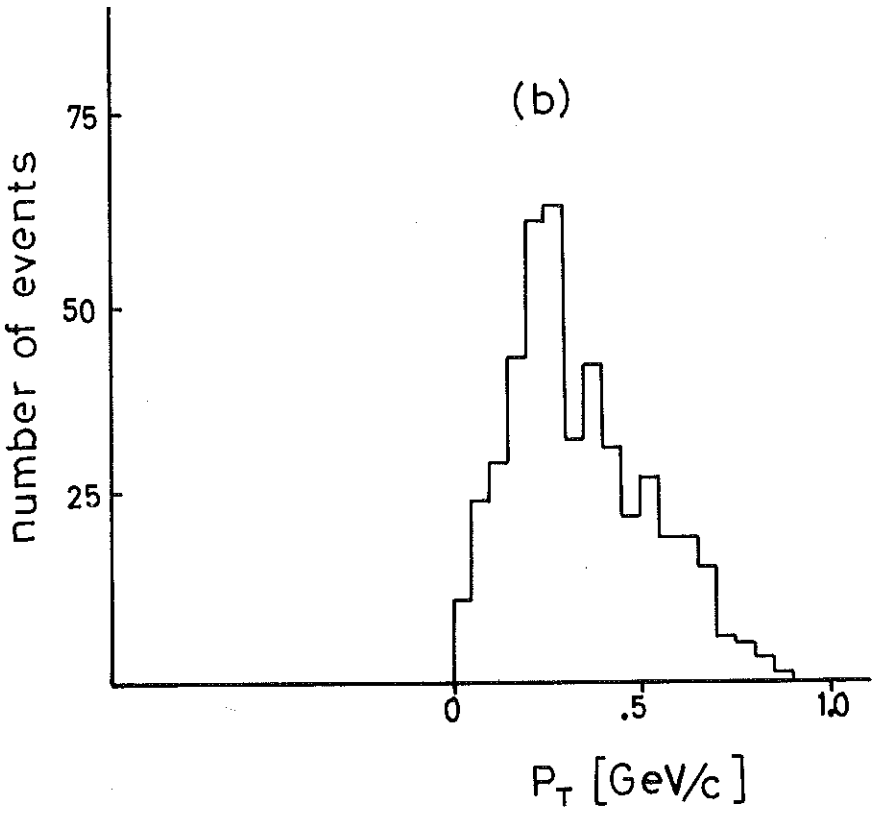
(b)
number of events
75
50
25
0
.5
1.0
P_T [GeV/c]

Fig 7

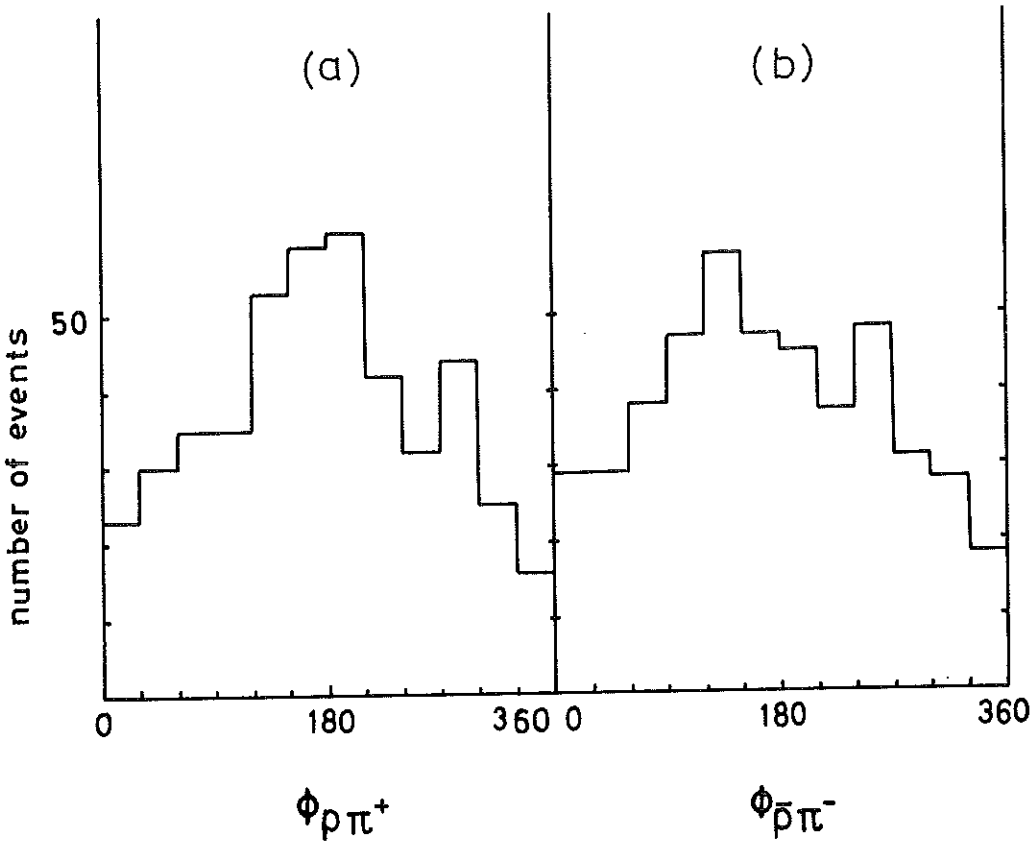
(a)
(b)
number of events
50
0
180
360
0
180
360
$\phi_{p\pi^+}$
$\phi_{\bar{p}\pi^-}$

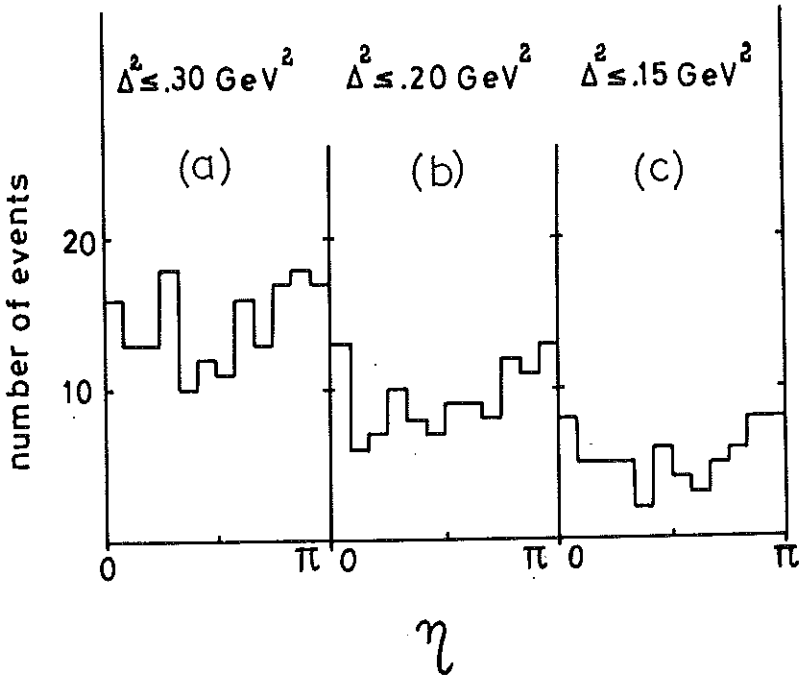
$\Delta^2 \leq .30\ GeV^2$
$\Delta^2 \leq .20\ GeV^2$
$\Delta^2 \leq .15\ GeV^2$
(a)
(b)
(c)
number of events
20
10
0
π
0
π
0
π
η

Fig 8, Fig 9

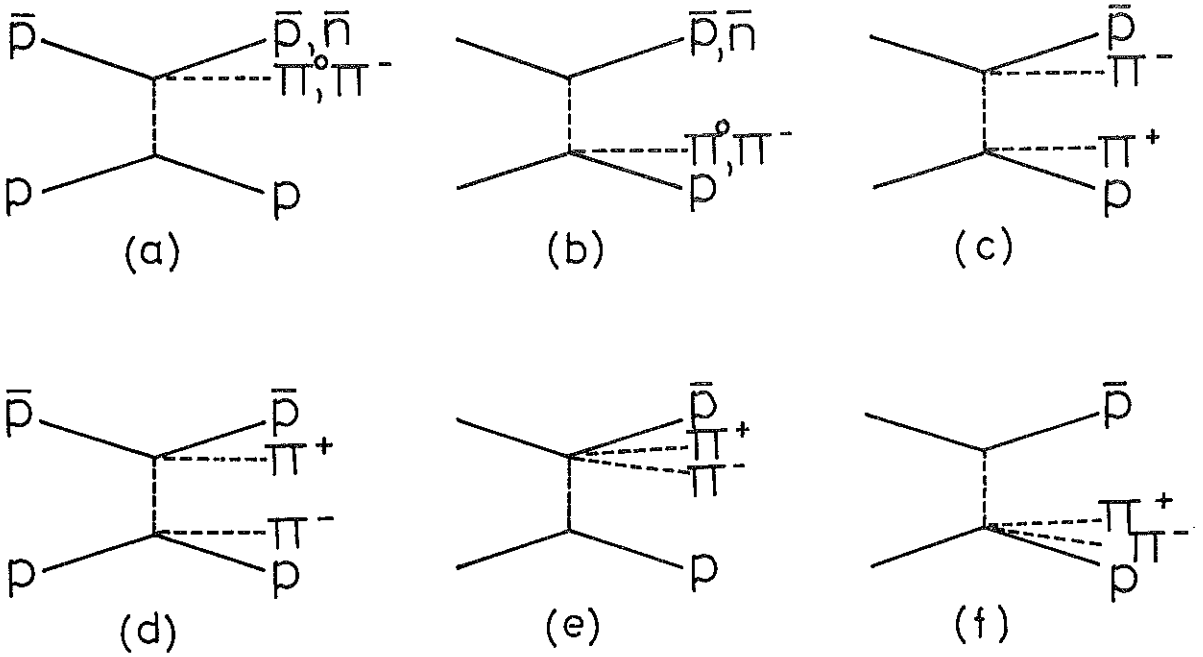

Fig 10

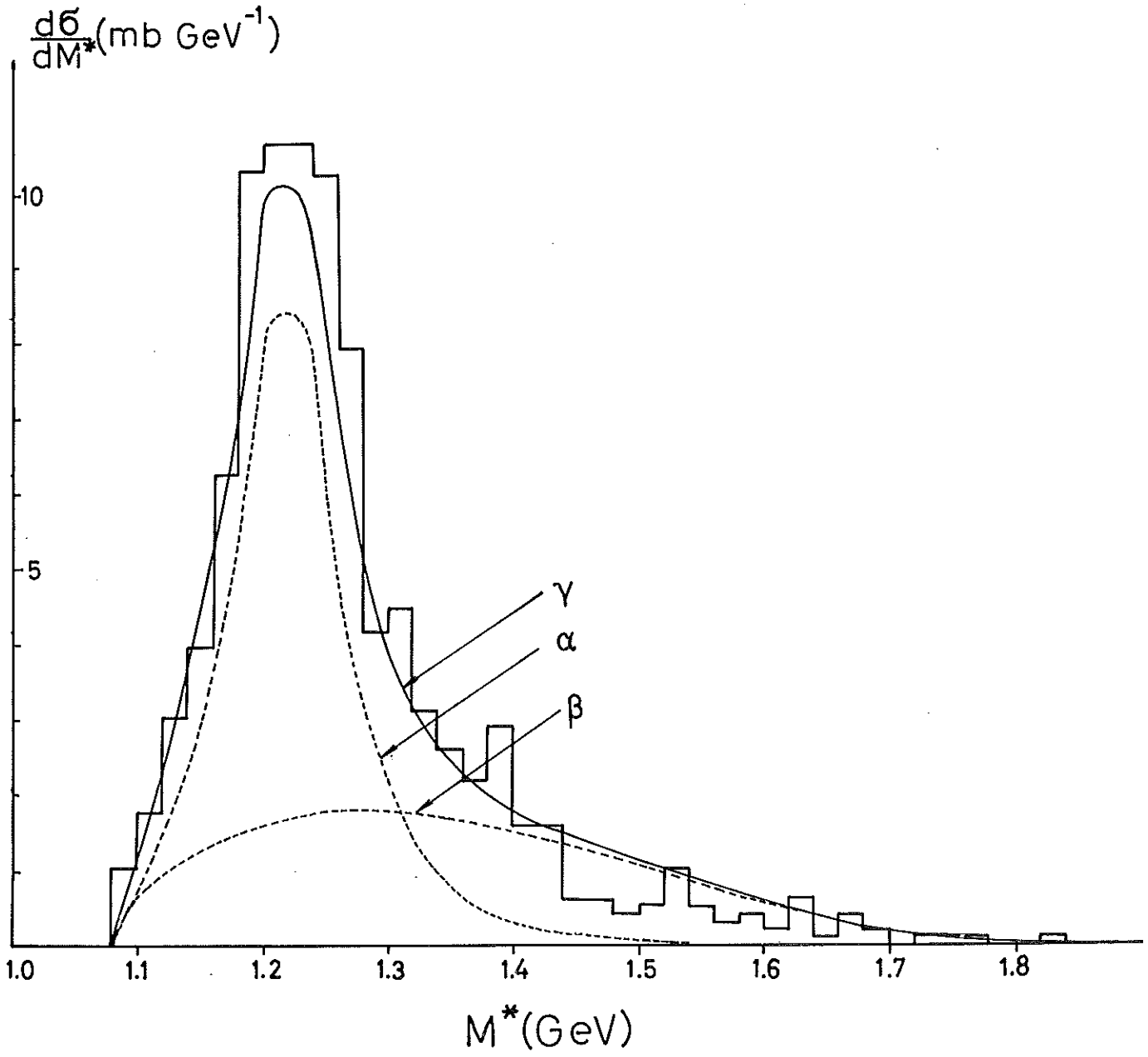

Fig. 11

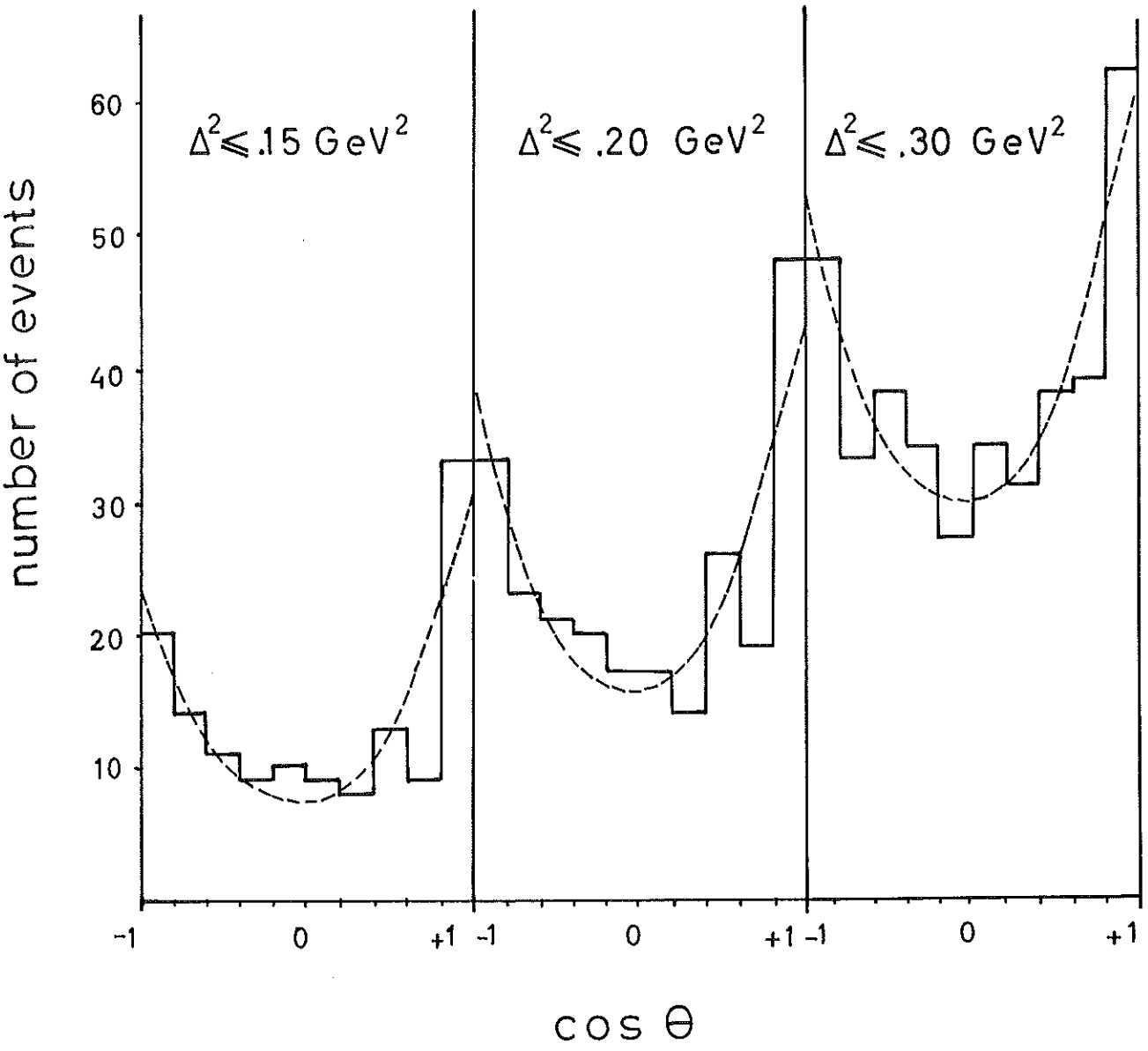
number of events
60
50
40
30
20
10
$\Delta^2 \leqslant .15\ GeV^2$
$\Delta^2 \leqslant .20\ GeV^2$
$\Delta^2 \leqslant .30\ GeV^2$
-1
0
+1
-1
0
+1
-1
0
+1
cos θ

Fig. 12